Suplementary Materials: Cross-Linked CoMoO4/rGO Nanosheets as Oxygen Reduction Catalyst

Jiaqi Fu [1], Jiang-Li Meng [1], Mei-Jie Wei [1], Hong-Ying Zang [1],*, Hua-Qiao Tan [1], Yong-Hui Wang [1],*, Haralampos N. Miras [2],* and Yang-Guang Li [1],*

[1] Key Laboratory of Polyoxometalate Science of Ministry of Education, Key Laboratory of Nanobiosensing and Nanobioanalysis at Universities of Jilin Province, Faculty of Chemistry, Northeast Normal University, Changchun 130024, China; fujq140@nenu.edu.cn (J.F.); mengjl480@nenu.edu.cn (J.-L.M.); weimj212@nenu.edu.cn (M.-J.W.); tanhq870@nenu.edu.cn (H.-Q.T.)

[2] School of Chemistry, The University of Glasgow, Galsgow G12 8QQ, UK

* Correspondence: zanghy100@nenu.edu.cn (H.-Y.Z.); wangyh319@nenu.edu.cn (Y.-H.W.); harism@chem.gla.ac.uk (H.N.M.); liyg658@nenu.edu.cn (Y.-G.L.); Tel.: +86-431-8568-4009 (H.-Y.Z. & Y.-H.W. & Y.-G.L.)
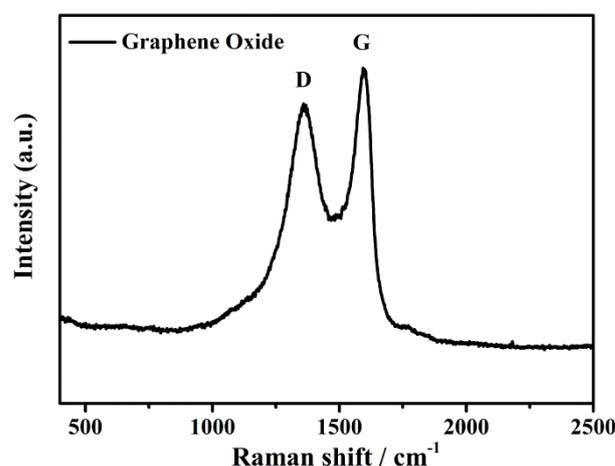
Figure S1. Raman spectra of graphene oxide.

1. Physical characterization

A JEOL JSM 4800F SEM (JEOL company, Shanghai, China) and an FEI Tecnai G2 TEM (transmission electron microscopy) (FEI company, Hillsborough County, Oregon State , United States of America) were used to visualize the morphologies and microstructures of CoMoO$_4$/rGO, rGO and CoMoO$_4$ samples. X-ray photoelectron spectroscopy (XPS) was tested by using an ESCALABMKII spectrometer with an Al-Ka (1486.6 eV) achromatic X-ray source (Thermo Fisher Scinentific, Waltham, MA, USA). Powder X-ray diffraction measurements were recorded on a Siemens D5005 diffractometer with Cu-Kα radiation (λ = 1.5418 Å) (Bruker , Aubrey, Texas , USA). Raman spectra were recorded with a LabRAM HR high-resolution Raman spectrometer (Horiba-Jobin Yvon) (Horiba-Jobin Yvon , Paris , France).

2. Electrochemical measurements

All the electrochemical tentatives were carried out on an electrochemical analysis station (CHI760E, Princeton) using a three-electrode cell. Rotating disk electrode (RDE, 5 mm diameter) or rotating ring disk electrode (RRDE, 5.61 mm diameter) was the working electrode, Ag/AgCl electrode and Pt mesh regarded as the reference electrode and counter electrode, respectively. To prepare the working electrode, 4.0 mg of the CoMoO$_4$/rGO catalyst was ultrasonically dissolved into 1.0 mL of aqueous solution including 0.05 wt % Nafion (V_{H_2O}: V $_{Nafion}$= 9:1) for 30 min.. The volume of catalyst ink was 10 μL for the RDE/RRDE examines the CV and LSV. The catalyst loading on rotating disk electrode was 0.254 mg/cm^2. As a comparison, the Pt/C working electrode was

made with the same method with the commercial Pt/C (20 wt %) powder instead of the CoMoO$_4$/rGO powder.

Before the test, high-purity N$_2$ or O$_2$ gas was injected into the alkaline solution for at least 30 min. In 0.1 M KOH, the Ag/AgCl electrode was calibrated with reversible hydrogen electrode (RHE), $E_{RHE} = E_{Ag/AgCl} + 0.059pH + 0.205$. Cyclic voltammetry (CV) and linear sweep voltammetry (LSV) tests were conducted with a scan rate of 10 mV s^{-1} and 5 mV s^{-1}, respectively. All LSV curves were presented without iR compensation.

For the RDE measurements, the LSV curves were inspected at different rotating speeds (100-2500 rpm). The electron transfer number (n) was computed using the Koutecky−Levich (K-L) equation [16, S1]:

$$j^{-1} = j_k^{-1} + (0.62nFC_o(D_o)^{2/3}v^{-1/6}\omega^{1/2})^{-1}$$

Where j is the measured current density, j_k is the kinetic current density. F is the Faraday constant (96485 C mol^{-1}). C_o is the bulk concentration of O$_2$ in 0.1 M KOH (1.2 × 10^{-3} mol L^{-1}). D_o is the diffusion coefficient of O$_2$ in 0.1 M KOH (1.9 × 10^{-5} cm^2 s^{-1}). v is the kinetic viscosity of the electrolyte (0.01 cm^2 s^{-1}), and ω is the electrode rotating rate.

For the RRDE measurements, the polarization curves were carried out at a rotating velocity of 1600 rpm, and the potential of the ring was fixed to 0.5 V (*vs.* Ag/AgCl). The electron transfer number (n) and the H$_2$O$_2$ yield were estimated as followed [S2]:

$$n = 4 \times \frac{I_d}{I_d + I_r/N} \tag{1}$$

$$H_2O_2\% = 200 \times \frac{I_r/N}{I_d + I_r/N} \tag{2}$$

where I$_r$ is the ring current and I$_d$ is the disk current. N is the collection efficiency (0.37).

The stability of the samples was evaluated by the chronoamperometric response (i.e., the *I–t* curve) at -0.2 V (*vs. E$_{Ag/AgCl}$*). The methanol tolerance examination was tested in O$_2$- purged 0.1 M KOH in the presence of 1.0 M methanol.

Table S1. Comparison of ORR activity parameters with other recently reported.

Catalyst	Electrolyte	Reference electrode employed	Onset Potential (V vs RHE)	References
CoMoO$_4$/rGO	0.1 M KOH	Ag/AgCl	0.89	This work
Co$_3$O$_4$/N-csCNT–GNR	0.1 M KOH	Ag/AgCl	0.89	[S3]
Co/N-C-800	0.1 M KOH	Ag/AgCl	0.834	[S4]
CoO@N/S-CNF	0.1 M KOH	Hg/HgO	0.84	[S5]
Co/CoNx/N-CNT/C	0.1 M KOH	Hg/HgO	0.90	[S6]
NPAC$_{Co}$	0.1 M KOH	Hg/HgO	0.87	[S7]
NiCo$_2$O$_4$–G	0.1 M KOH	Hg/HgO	0.871	[S8]
Fe/Co-NpGr	0.1 M KOH	Hg/HgO	0.93	[S9]
NiCoMnO$_4$/N-rGO	0.1 M KOH	Hg/HgO	0.92	[S10]
Co$_{0.25}$-N$_{0.32}$/C-800	0.1 M KOH	Hg/HgO	0.93	[S11]
Co$_{1-x}$S/N–S–G	0.1 M KOH	Ag/AgCl	0.978	[S12]
NiCo$_2$O$_4$/C	0.1 M KOH	Ag/AgCl	0.81	[S13]
Co$_3$O$_4$/N-rmGO	0.1 M KOH	Hg/HgO	0.88	[16]
Co@NSCNTs	0.1 M KOH	Ag/AgCl	0.90	[S14]
CoS$_2$(400)/N,S-GO	0.1 M KOH	Hg/HgO	0.97	[S15]
N-graphene/CNT	0.1 M KOH	Ag/AgCl	0.885	[S16]
CNT/BN	0.1 M KOH	Ag/AgCl	0.86	[S17]

Reference

S1. Zhong, H.; Li, K.; Zhang, Q.; Wang, J.; Meng, F.; Wu, Z.; Yan, J.; Zhang, X. In situ anchoring of Co_9S_8 nanoparticles on N and S co-doped porous carbon tube as bifunctional oxygen electrocatalysts. *NPG Asia Mater.* **2016**, *8*, e308.

S2. Liang, Y.; Wang, H.; Zhou, J.; Li, Y.; Wang, J.; Regier, T.; Dai, H. Covalent Hybrid of Spinel Manganese−Cobalt Oxide and Graphene as Advanced Oxygen Reduction Electrocatalysts. *J. Am. Chem. Soc.* **2012**, *134*, 3517–3523.

S3. Lu, X.; Chan, H. M.; Sun, C. L.; Tseng, C. M.; Zhao, C. Interconnected core–shell carbon nanotube–graphene nanoribbon scaffolds for anchoring cobalt oxides as bifunctional electrocatalysts for oxygen evolution and reduction. *J. Mater. Chem. A* **2015**, *3*, 13371–13376.

S4. Su, Y.; Zhu, Y.; Jiang, H.; Shen, J.; Yang, X.; Zou, W.; Chen, J.; Li, C. Cobalt nanoparticles embedded in N-doped carbon as an efficient bifunctional electrocatalyst for oxygen reduction and evolution reactions. *Nanoscale* **2014**, *6*, 15080–15089.

S5. Liu, T.; Guo, Y.; Yan, Y.; Wang, F.; Deng, C.; Rooney, D.; Sun, K. CoO nanoparticles embedded in three-dimensional nitrogen/sulfur co-doped carbon nanofiber networks as a bifunctional catalyst for oxygen reduction/evolution reactions. *Carbon* **2016**, *106*, 84–92.

S6. Zhong, H.; Luo, Y.; He, S.; Tang, P.; Li, D.; Alonso-Vante, N.; Feng, Y. Electrocatalytic Cobalt Nanoparticles Interacting with Nitrogen-Doped Carbon Nanotube in Situ Generated from a Metal−Organic Framework for the Oxygen Reduction Reaction. *ACS Appl. Mater. Interfaces* **2017**, *9*, 2541−2549.

S7. Zhang, M.; Jin, X.; Wang, L.; Sun, M.; Tang, Y.; Chen, Y.; Sun, Y.; Yang, X.; Wan, P. Improving biomass-derived carbon by activation with nitrogen and cobalt for supercapacitors and oxygen reduction reaction. *Appl. Surf. Sci.* **2017**, *411*, 251–260.

S8. Lee, D. U.; Kim, B. J.; Chen, Z. One-pot synthesis of a mesoporous $NiCo_2O_4$ nanoplatelet and graphene hybrid and its oxygen reduction and evolution activities as an efficient bi-functional electrocatalyst. *J. Mater. Chem. A* **2013**, *1*, 4754–4762.

S9. Palaniselvam, T.; Kashyap, V.; Bhange, S. N.; Baek, J. B.; Kurungot, S. Nanoporous Graphene Enriched with Fe/Co-N Active Sites as a Promising Oxygen Reduction Electrocatalyst for Anion Exchange Membrane Fuel Cells. *Adv. Funct. Mater.* **2016**, *26*, 2150–2162.

S10. Pendashteh, A.; Palma, J.; Anderson, M.; Marcilla, R. $NiCoMnO_4$ nanoparticles on N-doped graphene: Highly efficientbifunctional electrocatalyst for oxygen reduction/evolution reactions. *Appl. Catal. B* **2017**, *201*, 241–252.

S11. Zhang, R.; Li, Y.; Liu, L.; Jiang, M.; Wang, W. The active site exploration of Co-based non-precious metal electrocatalysts for oxygen reduction reaction. *Ionics* **2017**, *23*, 1849–1859.

S12. Qiao, X.; Jin, J.; Fan, H.; Li, Y.; Liao, S. In situ growth of cobalt sulfide hollow nanospheres embedded in nitrogen and sulfur co-doped graphene nanoholes as a highly active electrocatalyst for oxygen reduction and evolution. *J. Mater. Chem. A* **2017**, *5*, 12354–12360.

S13. Wang, J.; Wu, Z.; Han, L.; Lin, R.; Xin, H. L.; Wang, D. Hollow-Structured Carbon-Supported Nickel Cobaltite Nanoparticles as an Efficient Bifunctional Electrocatalyst for the Oxygen Reduction and Evolution Reactions. *ChemCatChem* **2016**, *8*, 736–742.

S14. Song, A.; Yang, W.; Yang, W.; Sun, G.; Yin, X.; Gao, L.; Wang, Y.; Qin, X.; Shao, G. Facile Synthesis of Cobalt Nanoparticles Entirely Encapsulated in Slim Nitrogen-Doped Carbon Nanotubes as Oxygen Reduction Catalyst. *ACS Sustain. Chem. Eng.* **2017**, *5*, 3973–3981.

S15. Ganesan, P.; Prabu, M.; Sanetuntikul, J.; Shanmugam, S. Cobalt Sulfide Nanoparticles Grown on Nitrogen and Sulfur Codoped Graphene Oxide: An Efficient Electrocatalyst for Oxygen Reduction and Evolution Reactions. *ACS Catal.* **2015**, *5*, 3625−3637.

S16. Wen, Z.; Ci, S.; Hou, Y.; Chen, J. Facile One-Pot, One-Step Synthesis of a Carbon Nanoarchitecture for an Advanced Multifunctonal Electrocatalyst. *Angew. Chem. Int. Ed.* **2014**, *53*, 6496 –6500.

S17. Patil, I. M.; Lokanathan, M.; Ganesan, B.; Swami, A.; Kakade, B. Carbon Nanotube/Boron Nitride Nanocomposite as a Significant Bifunctional Electrocatalyst for Oxygen Reduction and Oxygen Evolution Reactions. *Chem. Eur. J.* **2017**, *23*, 676–683.